

BLP-10 / ISS2008

Submitted 27 October 2008

Revised 13 January 2009

Enhancement of total trapped fluxes on $\phi 65$ mm GdBaCuO bulk by multi-pulse techniques

H. Fujishiro^a, K. Kakehata^a, T. Naito^a, Y. Yanagi^b, Y. Itoh^b

^a Faculty of Engineering, Iwate University, 4-3-5 Ueda, Morioka 020-8551, Japan

^b IMRA Material R&D Co. Ltd., 2-1 Asahi-cho, Kariya 448-0032, Japan

Abstract

We have investigated the total trapped flux $\Phi_T(z)$ on the $\phi 65$ mm GdBaCuO superconducting bulk as a function of distance z from the bulk surface magnetized by a successive pulse field application (SPA) with identical magnitude and subsequent iterative pulsed-field magnetization method with reducing the amplitude (IMRA) at various temperatures T_s . The $\Phi_T(z)$ value was enhanced by the IMRA process and reached 5.02 mWb on the bulk surface at $T_s=40$ K, which was about 1.7 times larger than that at the end of SPA. The $\Phi_T(4 \text{ mm})$ value at 40 K by the SPA+IMRA method was as high as $\Phi_T^{\text{FC}}(4 \text{ mm})$ by field cooled magnetization under $B_{\text{ex}}=3$ T at 48 K. The IMRA method is quite effective to enhance the Φ_T value for large superconducting bulks.

(125 words)

PACS: 74.25.Bt; 74.80.Bj; 74.60.Ge

Keywords: bulk superconductor; pulsed field magnetization; SPA+IMRA method;
total trapped flux density

*Prof. Hiroyuki Fujishiro

Faculty of Engineering, Iwate University, 4-3-5 Ueda, Morioka 020-8551, Japan

Phone: +81-19-621-6363

FAX: +81-19-621-6363

E-mail: fujishiro@iwate-u.ac.jp

ACCEPTED MANUSCRIPT

1. Introduction

To magnetize the REBaCuO superconducting bulks (RE: rare earth element) as a strong quasi-permanent magnet for practical applications such as a magnetic separation for environmental cleaning [1] and a drug delivery system (DDS) for medical applications [2], a pulsed-field magnetization (PFM) is suitable, instead of a conventional field cooled magnetization (FCM), because PFM is an inexpensive and mobile experimental setup. The trapped field B_T^P by PFM was, however, pretty smaller than the trapped field B_T^{FC} attained by FCM below 77 K because of the large temperature rise caused by the dynamical motion of magnetic fluxes in the bulk. Several approaches have been performed and succeeded to enhance B_T^P around 77 K such as an iteratively magnetizing pulsed-field method with reducing amplitude (IMRA) [3] and a multi-pulse technique with stepwise cooling (MPSC) [4]. We have systematically studied the time and spatial dependences of the temperature $T(t, x)$, the local field $B_L(t)$ and the trapped field B_T^P on the surface of cryo-cooled REBaCuO bulks [5]. To enhance B_T^P , we proposed a new PFM technique called a modified MPSC (MMPSC), which consisted of the two-stage temperature procedures [6]. Using the MMPSC method, we have succeeded in establishing a record of high-field trapping of $B_T^P=5.20$ T on the $\phi 45$ mm GdBaCuO bulk at 29 K to date [7], on which the maximum B_T^P of 3.6 T was attained by a single pulse application.

Recently, REBaCuO superconducting bulks with diameter larger than 60 mm are on the commercial market and even a single-grain bulk of 140 mm in diameter can be realized [8]. According to Bean's critical state model, a trapped field B_T at the bulk

center is proportional to the square of the diameter of the bulk disk d , and a total trapped flux density Φ_T is proportional to the cubic of d , if the critical current density J_c of the bulk material is identical. Another advantage of the large bulk magnet is that the magnetic field can reach a long distance, which is especially useful for the practical applications such as electric motor, generator and sputtering cathode.

We have investigated the trapped field characteristics on the $\phi 65$ mm GdBaCuO bulk by the successive pulse application (SPA) [9] and the MMPSC method [10]. The maximum trapped field on the $\phi 65$ mm bulk using SPA was as low as $B_T^P=1.9$ T at 40 K, but B_T^P was enhanced to 3.0 T using the MMPSC method, which were fairly smaller than those on the $\phi 45$ mm GdBaCuO bulk [7]. However, the Φ_T value for the large bulk is expected to enhance by the IMRA method because the Φ_T value of the $\phi 45$ mm GdBaCuO bulk had been about 30 % enhanced by the IMRA method after the termination of the MMPSC method [11].

In this paper, we perform the SPA+IMRA method on the $\phi 65$ mm GdBaCuO bulk under several temperatures T_s and applied pulse fields B_{ex} and investigate the effect of the enhancement of the Φ_T value on the multi pulse technique. We compare the Φ_T value by the SPA+IMRA method with the Φ_T^{FC} value obtained by the FCM.

2. Experimental Procedure

A $\phi 65$ mm GdBaCuO superconducting bulk disk of 20 mm in thickness (Nippon Steel) was used in this study. The trapped field B_T^{FC} by FCM was as high as 1.92 T at 77 K. The bulk was mounted on a soft iron yoke cylinder and tightly anchored onto the

cold stage of a Gifford-McMahon (GM) cycle helium refrigerator. The experimental setup around the bulk was described elsewhere [10]. The magnetizing solenoid coil, which generated the pulse field up to $B_{\text{ex}}=6.7$ T with a rise time of 12 ms and a duration of 100 ms, was placed outside the vacuum chamber, in which the central axis of the resulting field coincides with that of the bulk. The temperature T_s of the bulk was controlled over the range from 60 K to 40 K. Figure 1 shows the experimental sequence of the SPA+IMRA process. Three magnetic pulses (Nos. 1-3) with nearly the same amplitude $B_{\text{ex}}(\text{SPA}) (=B_1=B_2=B_3)$ were applied sequentially after re-cooling to T_s . From the No. 4 pulse, the IMRA process started, in which applied pulsed fields $B_{\text{ex}}(\text{IMRA})=B_n (>B_{n+1})$ were iteratively reduced down to 3.5 T by a 0.3 T step at constant T_s . Two-dimensional trapped field profile $B_T=B_T(z)$ was mapped at the distance z ($=0.5, 4$ and 8 mm) above the bulk surface, stepwise with a pitch of 1 mm by scanning an axial-type Hall sensor (F.W. Bell, BHA 921) inside the vacuum chamber using an x - y stage controller. The total amount of the total trapped magnetic flux density $\Phi_T=\Phi_T(z)$ was calculated by integrating the $B_T(z)$ value over the region where it was positive. The $B_T^{\text{FC}}(z)$ profiles by FCM were also measured at temperatures from 38 K to 77 K using a cryo-cooled superconducting magnet and $\Phi_T^{\text{FC}}(z)$ was estimated. During FCM, the static magnetic field of 3 T was decreased down to 0 T in 18 min.

3. Results and discussion

Figures 2(a) and 2(b), respectively, show the examples of the trapped field profile $B_T(0.5$ mm) for the first (No. 1) and the last (No. 13) pulse application in the

SPA+IMRA method ($T_s=40$ K, $BI=6.6$ T). For the No. 1 pulse, a concave B_T profile with nearly the axial symmetry can be observed and, for the No. 13 pulse, the B_T value entirely increased remaining the concave profile. Hereafter, we show the cross section of the B_T profile along the y -axis instead of the two-dimensional B_T profile, for simplicity.

Figure 3(a) shows the pulse number dependence of the cross section of the trapped field profile $B_T(0.5$ mm) for the SPA+IMRA method ($T_s=40$ K, $BI=6.6$ T). For the No. 1 pulse, the concave B_T profile can be seen, which was identical with the cross section of Fig. 2(a). The $B_T(0.5$ mm) value at the bulk periphery gradually increased with increasing pulse number. On the other hand, the $B_T(0.5$ mm) value at the bulk center only slightly increases. For the No. 13 pulse application ($BI=3.5$ T) in the IMRA process, the B_T increment at the bulk periphery seems to saturate. Figure 3(b) shows the trapped field profile $B_T(z)$ after applying the No. 13 pulse as a function of the distance z from the bulk surface. The $B_T(z)$ value at the bulk periphery drastically decreases with increasing z , but that at the bulk center remains constant. As a result, the trapped field profile changes from concave ($z=0.5$ mm) to trapezoid ($z=8$ mm).

Figure 4(a) shows the pulse number dependence of the $B_T(0.5$ mm) profiles for the SPA+IMRA method ($T_s=40$ K, $BI=5.4$ T). Since the applied pulse field BI is smaller than that in Fig. 3(a), only a small amount of the magnetic fluxes can intrude and can be trapped at the bulk center. In the IMRA process, the $B_T(0.5$ mm) value at the bulk periphery gradually increased and saturate with increasing pulse number. Figure 4(b) shows the $B_T(0.5$ mm) profiles for the SPA+IMRA method ($T_s=60$ K, $BI=6.6$ T) at

higher T_s . For the No. 1 pulse application, the $B_T(0.5 \text{ mm})$ profile shows nearly the cone-shaped one which results from the weaker pinning force than that at 40 K. The magnetic fluxes were additionally trapped both at the bulk periphery and bulk center in the IMRA process.

Figure 5 shows the total trapped fluxes $\Phi_T(0.5 \text{ mm})$ vs. the applied pulse field B_{ex} for each step in the SPA+IMRA method. In the figure, the numerals represent the pulse number n for each SPA+IMRA method. The $\Phi_T(0.5 \text{ mm})$ value gradually increases with increasing pulse number and then saturates for $B_{ex} < 4 \text{ T}$. The final $\Phi_T(0.5 \text{ mm})$ value depends on both T_s and BI values in the SPA process and increases with lowering T_s . It was found that the optimum BI value should exist to maximize the final $\Phi_T(0.5 \text{ mm})$ value at each T_s . In this study, we attained the maximum $\Phi_T(0.5 \text{ mm})$ value of 5.05 mWb for the $\phi 65 \text{ mm}$ GdBaCuO bulk using the SPA+IMRA method at $T_s=40 \text{ K}$ and at $BI=6.6 \text{ T}$. During the IMRA process, the $B_T(0.5 \text{ mm})$ value slightly increased from 1.17 T (No. 4 pulse) to 1.39 T (No. 13 pulse).

Figure 6 shows the total trapped fluxes $\Phi_T(z)$ obtained in this study, as a function of the distance z from the bulk surface for the SPA+IMRA process at $T_s=40 \text{ K}$ ($BI=6.6 \text{ T}$) and $T_s=60 \text{ K}$ ($BI=6.6 \text{ T}$). $\Phi_T(z)$ gradually decreased with increasing z ; $\Phi_T(0.5 \text{ mm})=5.05 \text{ mWb}$ and $\Phi_T(8 \text{ mm})=3.19 \text{ mWb}$ at $T_s=40 \text{ K}$ and at $BI=6.6 \text{ T}$. In the figure, the $\Phi_T^{FC}(z)$ values by FCM under 3 T and at $T=48, 60, 70$ and 77 K are also indicated. The $\Phi_T^{FC}(z)$ value increased with decreasing operating temperature T . It should be noted that the $\Phi_T(z)$ value by the SPA+IMRA method at 40 K is as high as the $\Phi_T^{FC}(z)$ value by FCM under 3 T at $T=48 \text{ K}$. If the FCM is operated under a static magnetic field higher

than 3 T, the $\Phi_T^{\text{FC}}(z)$ values are expected to increase. Since there is a possibility to make the bulk crash due to the hoop stress, we could not perform the FCM for $B > 3$ T at lower temperature. In Fig. 6, the $\Phi_T(5 \text{ mm})$ value magnetized by the MMPSC+IMRA process at $T_s=30$ K for the $\phi 45$ mm GdBaCuO bulk is also shown [11], on which $B_T(z=0 \text{ mm})=4.33$ T and $B_T(z=5 \text{ mm})=1.45$ T were realized by the MMPSC method. However, the $\Phi_T(z=5 \text{ mm})$ value was about a half of that for the $\phi 65$ mm bulk investigated in this study due to the smaller diameter of the bulk. The multi pulse technique such as the SPA+IMRA method is effective for the enhancement of the Φ_T value for the superconducting bulk as large as 65 mm in diameter, even though the B_T value at the bulk center is not so high.

In summary, the total trapped flux $\Phi_T(z)$ on the $\phi 65$ mm GdBaCuO superconducting bulk has been investigated as a function of distance z from the bulk surface using a successive pulse field application (SPA) with identical magnitude and subsequent iterative pulsed-field magnetization method with reducing the amplitude (IMRA) at $T_s=40$ and 60 K. The $\Phi_T(0.5 \text{ mm})$ value was enhanced by the IMRA method and reached 5.02 mWb on the bulk surface at $T_s=40$ K, which was about 1.7 times larger than that at the end of SPA. The $\Phi_T(4 \text{ mm})$ value by SPA+IMRA process was as high as the $\Phi_T^{\text{FC}}(4 \text{ mm})$ value by field cooled magnetization under 3 T at 48 K. The IMRA method is effective for the enhancement of the Φ_T value for large superconducting bulks. The Φ_T value closely depends on the shape of the trapped field profile at the end of the SPA process, the magnitude of the applied field B_{ex} during both SPA and IMRA processes, diameter of the bulk, the temperature T_s and so on. In this study, the

maximum B_{ex} was 6.6 T for the experimental setup reason and we cannot realize the convex shape at 40 K. Within our experimental conditions ($T_s \geq 40$ K, $B_{\text{ex}} \leq 6.6$ T), the maximum Φ_{r} value was realized under the concave trapped field profile. A detailed study is in progress.

This work is supported in part by a Grant-in-Aid for Scientific Research from the Ministry of Education, Culture, Sports, Science and Technology, Japan (No. 19560003).

References

- [1] H. Hayashi, K. Tsutsumi, N. Saho, N. Nishizima, K. Asano, *Physica C* **392-396** (2003) 745.
- [2] F. Mishima, S. Takeda, Y. Izumi, S. Nishijima, *IEEE Trans. Appl. Supercond.* **17** (2006) 2303.
- [3] Y. Yanagi, Y. Itoh, M. Yoshikawa, T. Oka, T. Hosokawa, H. Ishihara, H. Ikuta, U. Mizutani, *in: T. Yamashita, K. Tanabe (Eds.) Adv. Supercond. XII*, Springer-Verlag, Tokyo, 2000, P. 470.
- [4] M. Sander, U. Sutter, R. Koch, M. Klaser, *Supercond. Sci. Technol.* **13** (2000) 841.
- [5] H. Fujishiro, K. Yokoyama, T. Oka, K. Noto, *Supercond. Sci. Technol.* **17** (2004) 51.
- [6] H. Fujishiro, M. Kaneyama, T. Tateiwa, T. Oka, *Jpn. J. Appl. Phys.* **44** (2005) L1221.
- [7] H. Fujishiro, T. Tateiwa, A. Fujiwara, T. Oka, H. Hayashi, *Physica C* **445-448** (2006) 334.
- [8] N. Sakai, K. Inoue, S. Nariki, A. Hu, M. Murakami, I. Hirabayashi, *Physica C* **426-431** (2005) 515.
- [9] H. Fujishiro, T. Tateiwa, K. Kakehata, T. Hiyama, T. Naito, *Supercond. Sci. Technol.* **20** (2007) 1009.
- [10] H. Fujishiro, T. Tateiwa, K. Kakehata, T. Hiyama, T. Naito, Y. Yanagi, *Physica C* **468** (2008) 1477.
- [11] H. Fujishiro, T. Tateiwa, T. Hiyama, *Jpn. J. Appl. Phys.* **46** (2007) 4108.

Figure captions

Fig. 1. The experimental sequence of the SPA+IMRA method.

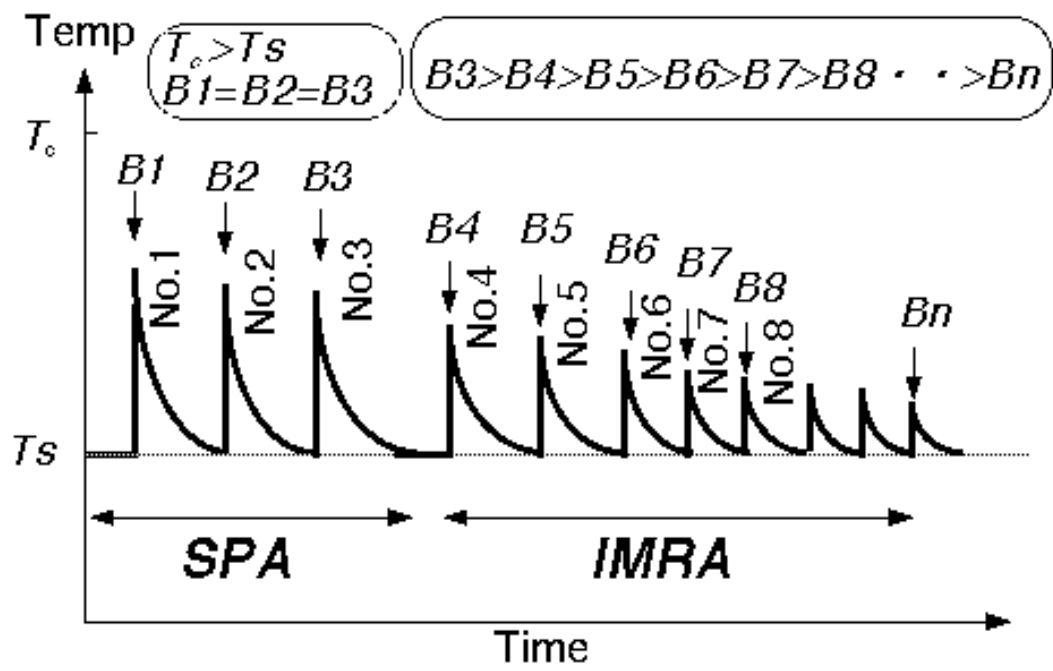
Fig. 2. The trapped field profiles $B_T(0.5 \text{ mm})$ at $T_s=40 \text{ K}$ after applying the (a) No. 1 pulse ($BI=6.6 \text{ T}$) in SPA and (b) No. 13 pulse ($BI=3.5 \text{ T}$) in IMRA.

Fig. 3. (a) The $B_T(0.5 \text{ mm})$ profile vs. the pulse number n and (b) $B_T(z)$ for the No. 13 pulse vs. the distance z from the bulk surface for the SPA+IMRA method ($T_s=40 \text{ K}$, $BI=6.6 \text{ T}$).

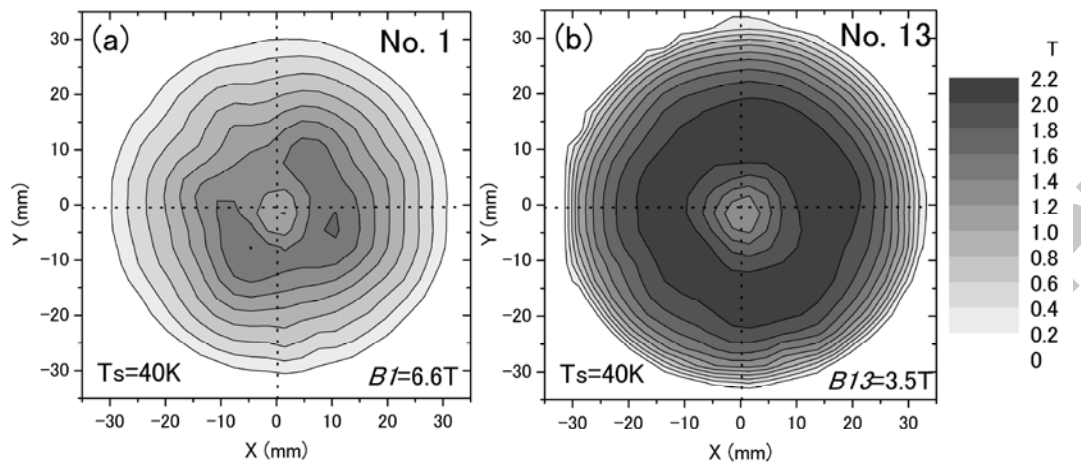
Fig. 4. The pulse number dependence of the $B_T(0.5 \text{ mm})$ profiles for the SPA+IMRA method ((a) $T_s=40 \text{ K}$, $BI=5.4 \text{ T}$ and (b) $T_s=60 \text{ K}$, $BI=6.6 \text{ T}$).

Fig. 5. The total trapped fluxes $\Phi_T(0.5 \text{ mm})$ vs. the applied pulse field B_{ex} for each condition in the SPA+IMRA method. In the figure, the numerals represent the pulse number n .

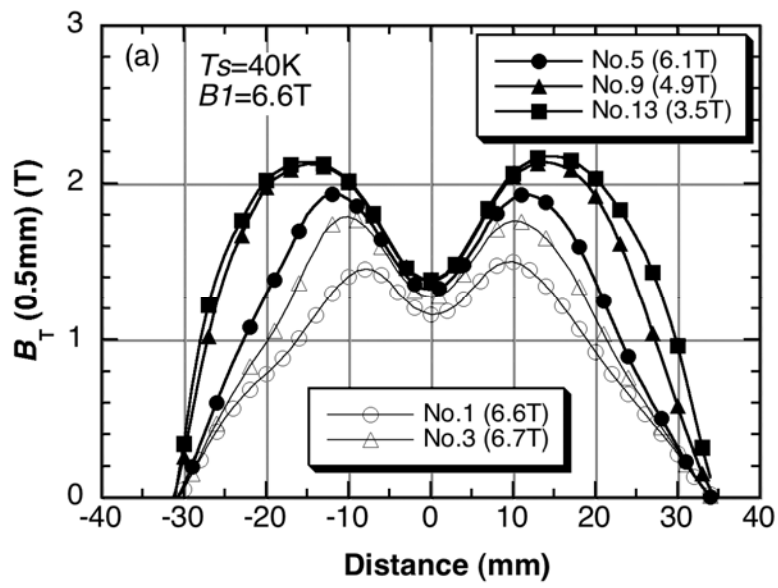
Fig. 6. The $\Phi_T(z)$ values as a function of the distance z from the bulk surface by the SPA+IMRA method at $T_s=40 \text{ K}$ and 60 K ($BI=6.6 \text{ T}$). $\Phi_T^{FC}(z)$ by FCM under the static magnetic field of 3 T at $T=48, 60, 70$ and 77 K and $\Phi_T(5 \text{ mm})$ by the MMPSC+IMRA method for the $\phi 45 \text{ mm}$ GdBaCuO bulk at $T_s=30 \text{ K}$ [11] are also indicated.

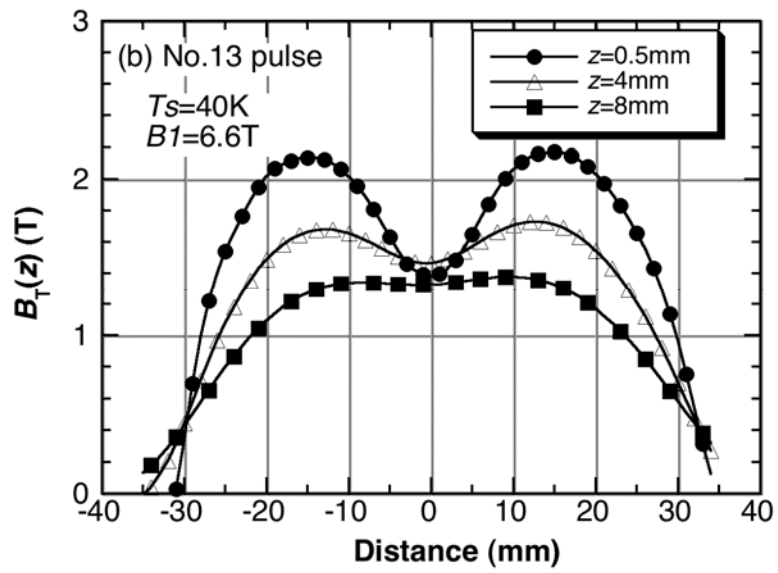


ACCEPTED MANUSCRIPT

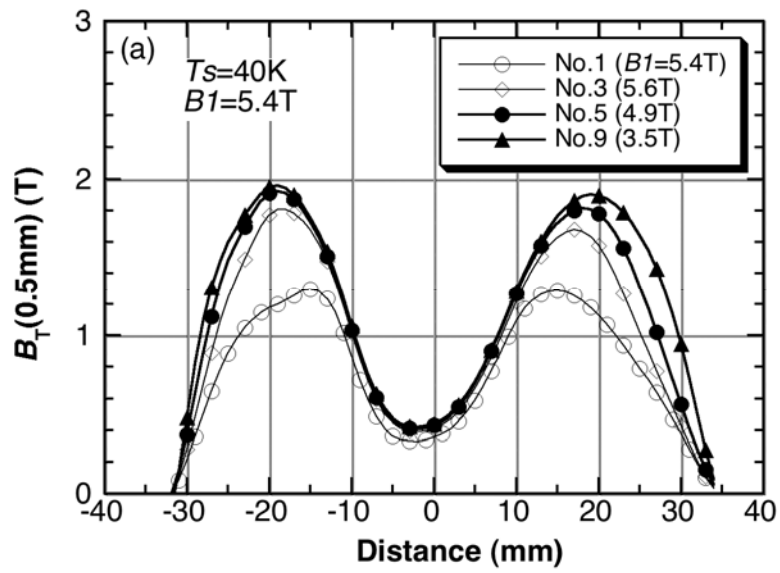


ACCEPTED MANUSCRIPT

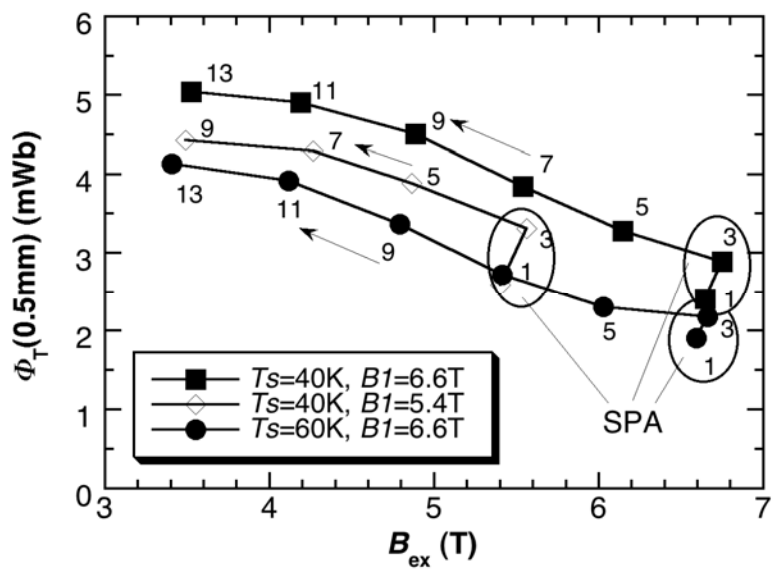




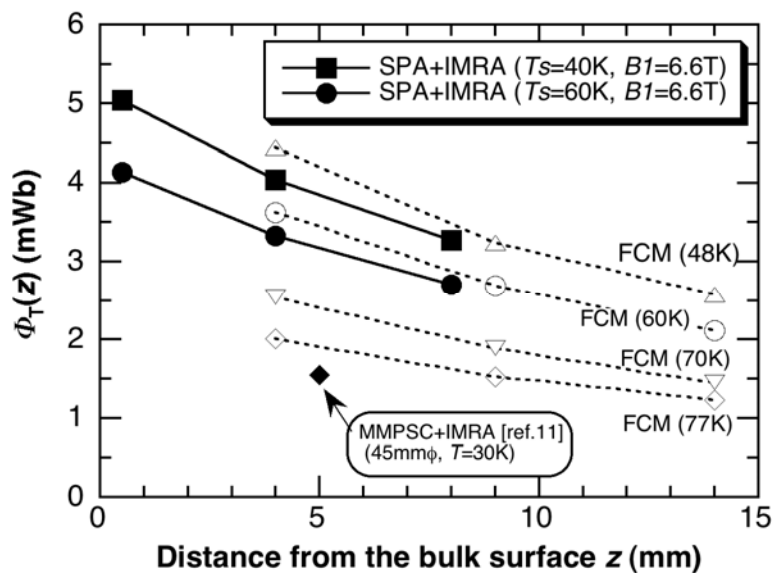
ACCEPTED MANUSCRIPT

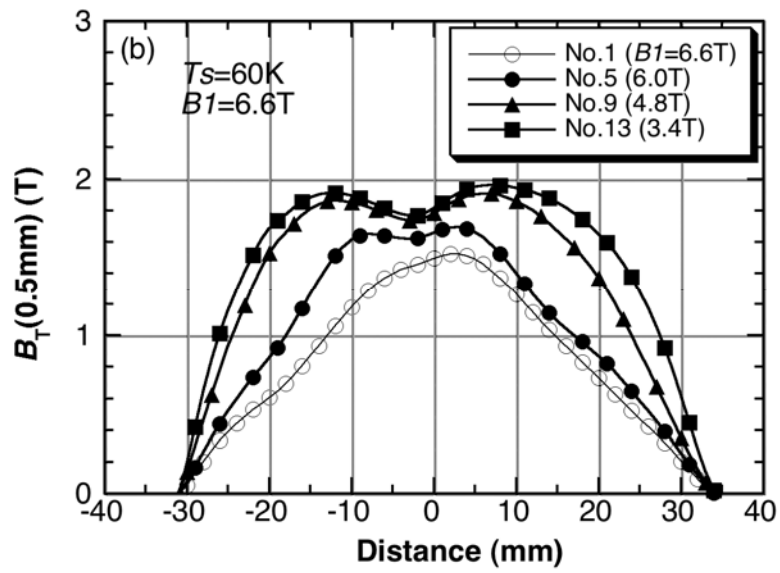


ACCEPTED MANUSCRIPT



ACCEPTED MANUSCRIPT





ACCEPTED MANUSCRIPT